p53 at the endoplasmic reticulum regulates apoptosis in a Ca^{2+}-dependent manner

Carlotta Giorgi[a,1], Massimo Bonora[a,1], Giovanni Sorrentino[b], Sonia Missiroli[a], Federica Poletti[a], Jan M. Suski[c], Fabian Galindo Ramirez[d,e], Rosario Rizzuto[f], Francesco Di Virgilio[a], Ester Zito[g], Pier Paolo Pandolfi[h,i], Mariusz R. Wieckowski[c], Fabio Mammano[d,e], Giannino Del Sal[b,i], and Paolo Pinton[a,2]

[a]Department of Morphology, Surgery and Experimental Medicine, Section of Pathology, Oncology and Experimental Biology, University of Ferrara, Ferrara 44121, Italy; [b]Laboratorio Nazionale del Consorzio Interuniversitario per le Biotecnologie (LNCIB), 34012 Trieste, Italy; [c]Department of Biochemistry, Nencki Institute of Experimental Biology, Warsaw 02-093, Poland; [d]Department of Physics and Astronomy, University of Padua, Padua 35129, Italy; [e]Venetian Institute of Molecular Medicine, Padua 35129, Italy; [f]Department of Biomedical Sciences, University of Padua, Padua 35131, Italy; [g]Dulbecco Telethon Institute, Istituto di Ricerche Farmacologiche Mario Negri, Milan 20156, Italy; [h]Cancer Genetics Program, Department of Medicine and Pathology, Beth Israel Deaconess Medical Center, Harvard Medical School, Boston, MA 02215; and [i]Dipartimento di Scienze della Vita, Univeristà degli Studi di Trieste, 34128 Trieste, Italy

Edited by Carol Prives, Columbia University, New York, NY, and approved December 30, 2014 (received for review June 9, 2014)

The tumor suppressor p53 is a key protein in preventing cell transformation and tumor progression. Activated by a variety of stimuli, p53 regulates cell-cycle arrest and apoptosis. Along with its well-documented transcriptional control over cell-death programs within the nucleus, p53 exerts crucial although still poorly understood functions in the cytoplasm, directly modulating the apoptotic response at the mitochondrial level. Calcium (Ca^{2+}) transfer between the endoplasmic reticulum (ER) and mitochondria represents a critical signal in the induction of apoptosis. However, the mechanism controlling this flux in response to stress stimuli remains largely unknown. Here we show that, in the cytoplasm, WT p53 localizes at the ER and at specialized contact domains between the ER and mitochondria (mitochondria-associated membranes). We demonstrate that, upon stress stimuli, WT p53 accumulates at these sites and modulates Ca^{2+} homeostasis. Mechanistically, upon activation, WT p53 directly binds to the sarco/ER Ca^{2+}-ATPase (SERCA) pump at the ER, changing its oxidative state and thus leading to an increased Ca^{2+} load, followed by an enhanced transfer to mitochondria. The consequent mitochondrial Ca^{2+} overload causes in turn alterations in the morphology of this organelle and induction of apoptosis. Pharmacological inactivation of WT p53 or naturally occurring p53 missense mutants inhibits SERCA pump activity at the ER, leading to a reduction of the Ca^{2+} signaling from the ER to mitochondria. These findings define a critical nonnuclear function of p53 in regulating Ca^{2+} signal-dependent apoptosis.

p53 | endoplasmic reticulum | mitochondria-associated membranes | calcium | apoptosis

The master tumor suppressor p53 is the hub of numerous signaling stress pathways that control cell fate (1). The inactivation of p53 function is a pivotal aspect of tumor formation in different human cancers. Its activity is crucial for regulating efficient cell death in cancer cells upon cellular stress (1) evoked by chemotherapeutic drugs or radiation. Many cancer cells, however, contain a mutant *TP53* gene or a nonfunctional p53 protein and are thus unable to respond efficiently to these treatments. Indeed, more than 50% of human cancers harbor somatic *p53* gene mutations (2). In addition to sporadic tumors, inherited heterozygous loss-of-function mutations in *TP53* cause Li–Fraumeni syndrome, which confers a high familial risk of various types of cancer (3). However, the mechanisms by which wild-type p53 suppresses tumor growth and influences the response to drug treatment by mediating apoptosis are not yet fully understood.

Two pools of p53, cytoplasmic and nuclear, have been well-established to independently respond to stress (4) through transcription-dependent and -independent mechanisms (5, 6), both of which are regulated by posttranslational modifications that allow its accumulation and the full activation of its proapoptotic functions (7).

The cytoplasm is the main source of p53 involved in the nontranscriptional pathway through mitochondrial translocation, whereas the nuclear p53 pool is responsible for transcription-dependent mechanisms (4, 6, 7).

We recently demonstrated the unexpected localization of the promyelocytic leukemia protein (PML) at the endoplasmic reticulum (ER) and at mitochondria-associated membranes (MAMs) (8), a specialized domain of close contact between the ER and mitochondria that is involved in maintaining a dynamic cross-talk between the two organelles (9). PML is a tumor suppressor that physically interacts and synergizes with p53 during apoptosis induction (10). ER–mitochondrial cross-talk is fundamental for the up-regulation of mitochondrial metabolism in stimulated cells (11) and plays a key role in decoding Ca^{2+}-mediated apoptotic signals (12–16). The down-regulation of ER–mitochondrial Ca^{2+} transfer caused by B-cell lymphoma 2 (Bcl-2) overexpression or PML impairment is important for the antiapoptotic effects of these proteins (17).

Recent studies have suggested that p53 participates in apoptosis induction by acting directly at mitochondria. Because p53 can mediate apoptosis without its DNA-binding domain (the domain proposed to be fundamental for the targeting of p53 to mitochondria), the mitochondrial localization of p53 is likely not the only transcription-independent mechanism by which p53 promotes apoptosis (18).

Significance

Accumulating evidence has underscored the role of cytosolic p53 in promoting cell death. Different reports have revealed that p53 participates in apoptosis induction by acting directly at mitochondria. However, because p53 can mediate apoptosis without its DNA-binding domain (the domain proposed to be fundamental for the targeting of p53 to mitochondria), the mitochondrial localization of p53 is likely not the only transcription-independent mechanism by which p53 promotes apoptosis. Here we demonstrate that p53 at the endoplasmic reticulum (ER) and at mitochondria-associated membranes, interacting with sarco/ER Ca^{2+}-ATPase pumps, modulates ER–mitochondria cross-talk and, in turn, Ca^{2+}-dependent apoptosis.

Author contributions: C.G., M.B., and P.P. designed research; C.G., M.B., G.S., S.M., F.P., J.M.S., F.G.R., and E.Z. performed research; C.G., M.B., G.S., S.M., F.P., J.M.S., F.G.R., R.R., F.D.V., E.Z., P.P.P., M.R.W., F.M., G.D.S., and P.P. analyzed data; and C.G., G.D.S., and P.P. wrote the paper.

The authors declare no conflict of interest.

This article is a PNAS Direct Submission.

[1]C.G. and M.B. contributed equally to this work.

[2]To whom correspondence should be addressed. Email: pnp@unife.it.

This article contains supporting information online at www.pnas.org/lookup/suppl/doi:10.1073/pnas.1410723112/-/DCSupplemental.

CELL BIOLOGY

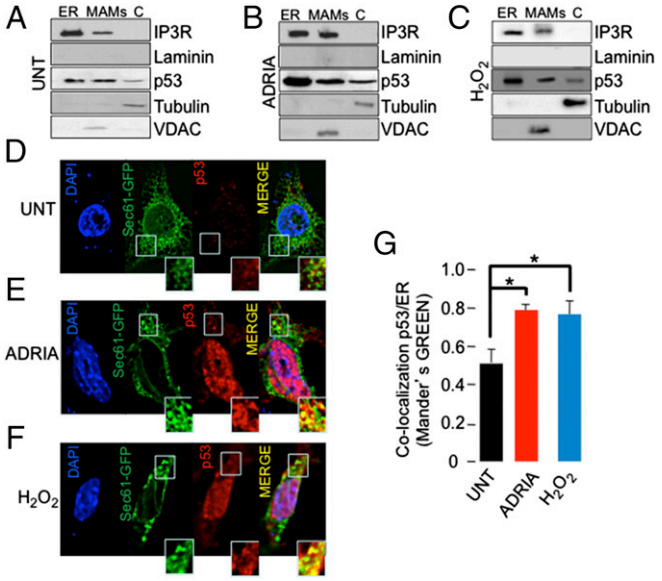

Fig. 1. p53 localizes at the ER and MAMs. (*A–C*) Detection of p53 by immunoblotting in HCT-116 $p53^{+/+}$ fractions. (*A*) p53 localization in untreated condition (UNT). Accumulation of p53 at the ER and MAMs in HCT-116 $p53^{+/+}$ cells after adriamycin (ADRIA) induction (1 μM, 6 h) (*B*) or after H_2O_2 treatment (500 μM, 6 h) (*C*). (*D–F*) Colocalization of p53 (red) and Sec61-GFP (used as ER marker; green) in $p53^{+/+}$ MEFs under untreated conditions (UNT) (*D*) and after ADRIA (*E*) or H_2O_2 (*F*). (*Insets*) A higher magnification of the images is presented. (*G*) p53 activation increased its ER colocalization. Colocalization of p53 and ER in $p53^{+/+}$ MEFs quantified as the proportion of total ER marker overlapping the p53 signal (by Mander's coefficient colocalization method). To allow for a better appreciation of colocalization of p53 with the ER, a cytoplasmic portion was selected and the contrast was increased. Bars, SEM; $*P < 0.05$.

Here we investigated and discuss whether an extranuclear localization of p53 could mediate its tumor-suppressive function through a nontranscriptional, Ca^{2+}-dependent pathway.

Results

p53 Accumulation at the ER/MAM Compartments After Anticancer Treatments Enhances Cell Death. To establish whether another nonmitochondrial p53 aspect could be involved in a nontranscriptional proapoptotic pathway, we verified the intracellular localization of p53 using biochemical and immunofluorescence techniques. Using a previously described subcellular fractionation protocol (19), we purified ER and MAM fractions from primary mouse embryonic fibroblasts (MEFs) and the human colon cancer HCT-116 $p53^{+/+}$ cell line. Similar to PML, p53 was localized to the ER and MAMs as well as the cytosolic fraction (Fig. 1*A* and Fig. S1*A*) under untreated conditions.

Therefore, we investigated whether adriamycin (ADRIA), a chemotherapeutic agent, or H_2O_2, an oxidative stress mediator, would change the subcellular localization of p53. An enrichment at the ER/MAMs was detected after p53 induction by either treatment (Fig. 1 *B* and *C* and Fig. S1 *B* and *C*). We confirmed p53 accumulation at the ER/MAMs by immunofluorescence using digital imaging 3D deconvolution (Fig. 1 *D–F*). The colocalization of p53 and the ER was analyzed in $p53^{+/+}$ MEFs as an overlap between the p53 and ER-marker (Sec61b-GFP) signals. The suitability of a colocalization analysis was verified by sampling the cytoplasmic portion of each cell and performing the randomized Costes et al. method (20). In all of the analyzed samples, the colocalization probability was higher than 99%. As expected, the overlap of p53 signal and ER-marker signal was increased in response to stress (Fig. 1*G*).

MEFs have previously been shown to be resistant to apoptosis induced by thapsigargin (TG) in the absence of p53 (21). In addition, p53 localizes to the ER/MAM compartments. Therefore, we investigated whether p53 could be a fundamental component of the ER stress-induced apoptotic pathway. Using different ER-stress inducers, we showed a marked reduction in the number of apoptotic cells in $p53^{-/-}$ MEFs compared with wild-type (WT) cells using flow cytometry analysis (Fig. 2 *A* and *B*), cytochrome *c* release (Fig. 2 *C* and *D*), and automated cell analysis based on morphological parameters and propidium iodide staining (Fig. 2*E*). Apoptotic cell death, evoked by H_2O_2, was blocked in cells pretreated with a caspase inhibitor (Fig. 2*F*) but enhanced after ADRIA-induced p53 accumulation at the ER/MAMs (Fig. 2 *G–I*).

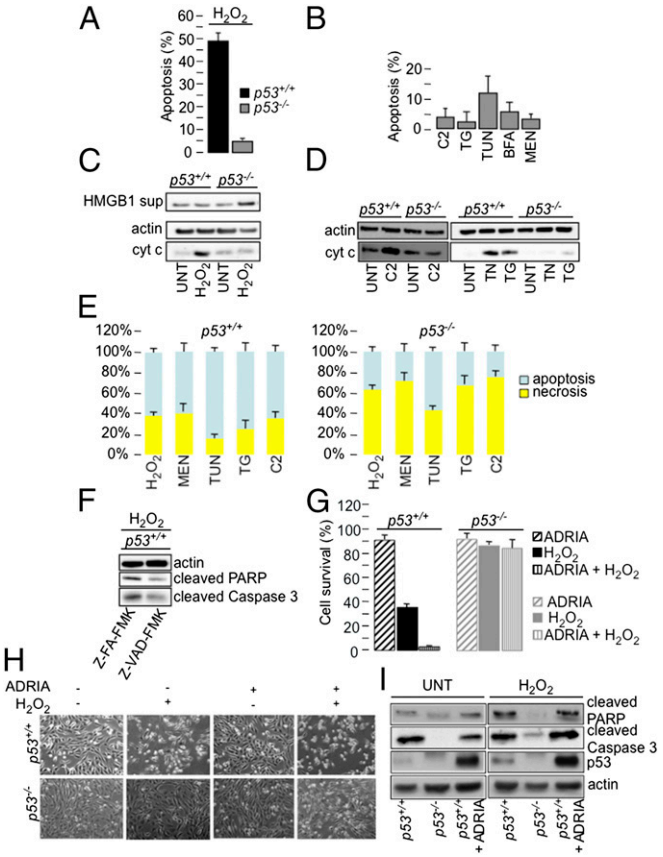

Fig. 2. Activation and accumulation of p53 at the ER/MAMs render cells more prone to death. (*A* and *B*) Percentage of apoptosis induced by (*A*) H_2O_2 (500 μM, 12 h) in $p53^{+/+}$ or $p53^{-/-}$ MEFs or (*B*) ceramide (C2; 60 μM, 12 h), thapsigargin (TG; 2 μM, 12 h), tunicamycin (TUN; 6 μM, 12 h), brefeldin A (BFA; 5 mg/mL, 12 h), or menadione (MEN; 15 μM, 12 h) in $p53^{-/-}$ MEFs. The data show the percentage of cell death in the whole cell population negative for annexin-V-FITC and propidium iodide (PI) staining, as analyzed by flow cytometry. (*C*) Detection of cytosolic cytochrome *c* release and supernatant HMGB1 release (a necrotic marker) by immunoblotting in $p53^{+/+}$ or $p53^{-/-}$ MEFs treated with H_2O_2 (500 μM, 12 h) compared with the untreated condition. Actin was used as a loading control for the cytosolic fraction. (*D*) Cytosolic cytochrome *c* release in $p53^{+/+}$ and $p53^{-/-}$ MEFs treated with C2 (60 μM, 12 h), TUN (6 μM, 12 h), or TG (2 μM, 12 h). (*E*) Percentage of apoptosis versus necrosis analyzed by automated imaging and cell scoring based on morphological parameters and PI staining in $p53^{+/+}$ and $p53^{-/-}$ MEFs treated with H_2O_2 (500 μM, 12 h), MEN (15 μM, 12 h), TUN (6 μM, 12 h), TG (2 μM, 12 h), or C2 (60 μM, 12 h). (*F*) Z-VAD-FMK treatment inhibits cell death in $p53^{+/+}$ MEFs (H_2O_2, 500 μM, 6 h). (*G*) Quantification of cell survival induced by H_2O_2 (500 μM, 12 h) through automated nucleus count analysis. Bars, SEM. (*H*) Representative microscopic fields of $p53^{+/+}$ and $p53^{-/-}$ MEFs under untreated conditions, pretreated with ADRIA (1 μM, 6 h) and then H_2O_2 (1 mM, 12 h). (*I*) Detection of apoptosis by immunoblotting in $p53^{+/+}$ and $p53^{-/-}$ MEFs and $p53^{+/+}$ pretreated with ADRIA (1 μM, 6 h) under untreated conditions and with H_2O_2 (500 μM, 6 h).

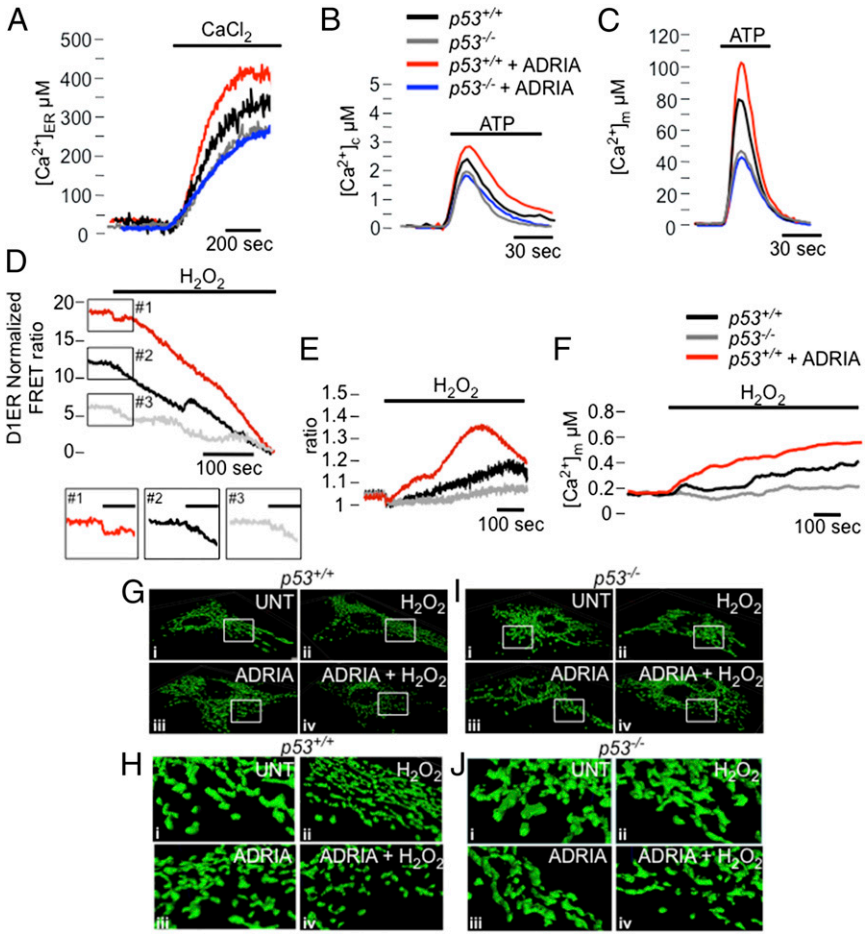

Fig. 3. Deregulation of Ca^{2+} homeostasis after p53 induction is a stress signal for mitochondrial structure and a trigger for apoptosis. (*A–C*) Measurements of $[Ca^{2+}]$ using recombinant aequorin upon agonist stimulation (100 μM ATP) in the ER (*A*), cytosol (*B*), and mitochondria (*C*). (*D*) ER Ca^{2+} release induced by H_2O_2 measured using a FRET-based Ca^{2+}-sensitive D1ER-YC4.3 probe; the normalized FRET ratio of D1ER-YC4.3 was assumed as the intraluminal $[Ca^{2+}]$. (*Insets*) A magnified portion of the first 2 min of the recording as basal. (*E*) Cytosolic Ca^{2+} response induced by H_2O_2 (2 mM) in MEFs loaded with the Ca^{2+}-sensitive fluorescent dye Fura-2. The kinetic behavior of the $[Ca^{2+}]_c$ (Ca^{2+} concentration within cytoplasm) response is presented as the ratio of fluorescence at 340 nm/380 nm. (*F*) Analysis of $[Ca^{2+}]_m$ (Ca^{2+} concentration within mitochondrial matrix) during oxidative stress upon H_2O_2 stimulation (2 mM). Isosurface rendering of representative $p53^{+/+}$ (*G* and *H*) and $p53^{-/-}$ (*I* and *J*) MEFs expressing mitochondrial GFP in basal conditions (UNT), after adriamycin (1 μM, 6 h), and/or H_2O_2 exposure (500 μM, 3 h). (*H* and *J*) High-resolution imaging of mitochondrial fragmentation during p53 activation and oxidative stress induction in $p53^{+/+}$ and $p53^{-/-}$ MEFs.

p53 Induction at the ER/MAMs Regulates Ca^{2+} Homeostasis, Allowing for Mitochondrial Fragmentation and Apoptosis. The key process connecting apoptosis to the ER–mitochondrial interaction is an alteration in Ca^{2+} homeostatic mechanisms (13, 22, 23) that results in massive and/or prolonged mitochondrial Ca^{2+} overload (13, 24, 25). We thus examined the effect of p53 down-regulation and induction on Ca^{2+} homeostasis. Using recombinant aequorin probes (26), $[Ca^{2+}]$ was measured selectively in the cytosol and in organelles acting as a source (ER) or target (mitochondria) of cellular Ca^{2+} signals. A striking difference was evident in $[Ca^{2+}]_{ER}$ (Ca^{2+} concentration within ER lumen) steady-state levels (Fig. 3*A*). After p53 induction by ADRIA the $[Ca^{2+}]_{ER}$ was higher, whereas the loss of p53 caused a reduction in the $[Ca^{2+}]_{ER}$ compared with WT. Representative traces are shown in the figures whereas the full dataset is included in Table S1.

In agreement with the $[Ca^{2+}]_{ER}$ data, the $[Ca^{2+}]$ increases evoked by agonist stimulation (ATP) in the cytosol and in the mitochondria were significantly higher after ADRIA treatment and lower in $p53^{-/-}$ MEFs than in WT MEFs (Fig. 3 *B* and *C*). Similarly, increased Ca^{2+} traffic from the ER to the mitochondria was observed in both HeLa cells overexpressing a WT p53 construct (4) (Fig. S2 *A–C*) and $p53^{+/+}$ HCT-116 cells upon ADRIA treatment (Fig. S2*D*), as well as in $p53^{-/-}$ MEFs after the reintroduction of WT p53 (Fig. S2*E*). In contrast, ADRIA treatment in $p53^{-/-}$ MEFs had no effect on Ca^{2+} homeostasis (Fig. 3 *A–C*, blue traces). The effect of p53 at the ER was also confirmed by analyzing mitochondrial Ca^{2+} uptake in permeabilized cells exposed to the same $[Ca^{2+}]$. Under these conditions, no differences were observed with regard to the p53 levels (Fig. S2*F*), indicating that the p53-dependent Ca^{2+} responses previously described were due to alterations of the source of the Ca^{2+} signals, the ER.

As mentioned above, there is a strong agreement in the literature linking Ca^{2+} transfer from the ER to the mitochondria and the effects of apoptotic stimuli (13, 22, 23, 25). Therefore, we investigated whether the absence or the induction of p53 could alter $[Ca^{2+}]_m$ after apoptotic stimuli. We observed that the agonist-dependent mitochondrial Ca^{2+} response, after the oxidative apoptotic inducer H_2O_2, was reduced proportional to p53 expression (Fig. S3*A*). Using the ER-targeted, FRET-based Ca^{2+}-sensitive D1ER-YC4.3 probe, we measured the effect of p53 on the progressive release of Ca^{2+} from the ER caused by H_2O_2. The normalized FRET ratio (proportional to $[Ca^{2+}]_{ER}$) was observed to correlate with p53 levels (Fig. 3*D* and Fig. S3*B*). Administration of H_2O_2 caused a progressive depletion of Ca^{2+} from the ER (as revealed by a reduction in the normalized FRET ratio) with consequent increases in $[Ca^{2+}]$ in the cytosol (Fig. 3*E* and Fig. S3*C*) and mitochondria (Fig. 3*F* and Fig. S3*D*). Furthermore, this event appeared to be proportional to p53 levels.

To assess whether the observed ER Ca^{2+} overload is a proapoptotic condition, we analyzed the mitochondrial morphology after apoptotic stress induction. The mitochondria of WT p53 and $p53^{-/-}$ MEFs were labeled with targeted GFP, and the mitochondrial structure was evaluated by confocal microscopy. Treatment with H_2O_2 for 3 h caused a strong reduction in the average mitochondrial volume in WT cells, as expected, upon network breakage (Fig. 3 *G*, *i* and *ii*, and *H*, *i* and *ii*, and Fig. S4 *A* and *B*). The induction of p53 by ADRIA alone did not significantly affect mitochondrial morphology (Fig. 3 *G*, *iii*, and *H*, *iii*, and Fig. S4 *A* and *B*), whereas ADRIA treatment followed by H_2O_2 exposure induced a stronger increase in the fragmentation index value (Fig. 3 *G*, *iv*, and *H*, *iv*, and Fig. S4 *A* and *B*) compared with H_2O_2 alone. $p53^{-/-}$ cells treated with H_2O_2 did not show significant changes in the mitochondrial network (Fig. 3 *I* and *J* and Fig. S4 *C* and *D*).

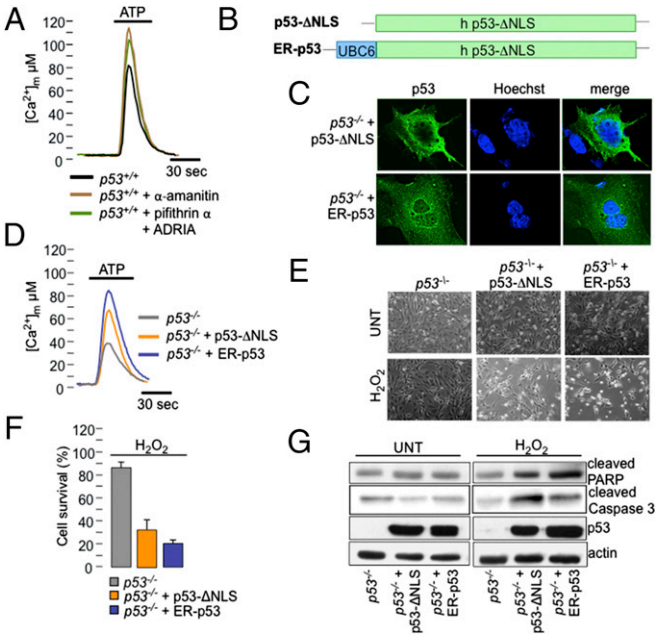

Fig. 4. p53 controls mitochondrial Ca^{2+} homeostasis and, in turn, apoptotic sensitivity from ER/MAM compartments. (*A*) Agonist-dependent $[Ca^{2+}]_m$ response in $p53^{+/+}$ MEFs after pharmacological block of the transcriptional arm of p53. (*B*) Schematic representation of p53-ΔNLS and ER-p53 chimeras. (*C*) Immunofluorescence images of $p53^{-/-}$ MEF cells expressing the p53-ΔNLS or ER-p53 constructs stained with anti-p53 antibody (green) and Hoechst (nuclear marker). (*D*) Mitochondrial Ca^{2+} response in $p53^{-/-}$ MEFs after the reintroduction of an ER-targeted chimera, ER-p53 or p53-ΔNLS. (*E*) Representative microscopic fields, from three independent experiments, of $p53^{-/-}$ MEFs expressing p53-ΔNLS and ER-p53 before and after H_2O_2 treatment (1 mM, 12 h). (*F*) Evaluation of cell-death induction by H_2O_2 (500 μM, 12 h) through automated nucleus count analysis in $p53^{-/-}$ MEFs, $p53^{-/-}$ MEFs expressing ER-p53, and $p53^{-/-}$ MEFs expressing p53-ΔNLS. Bars, SEM. (*G*) Analysis of apoptotic markers by immunoblot in $p53^{-/-}$ MEFs and $p53^{-/-}$ MEFs expressing p53-ΔNLS and ER-p53 under untreated conditions and after H_2O_2 treatment (500 μM, 6 h).

Naturally Occurring p53 Mutants Lose Their Ability to Modulate Ca^{2+} Responses. To exclude the possibility that a transcription-dependent pathway of p53 accounts for its effect on Ca^{2+} homeostasis (and, in turn, on the sensitivity of ER-stress apoptotic stimuli), we used different strategies: specific drugs blocking the transcriptional arm of p53 (Fig. 4*A*) and p53-targeted chimeras, p53-ΔNLS (a nuclear import-deficient p53 mutant; Fig. 4 *B* and *C*) and ER-p53 (a chimera containing the human p53-ΔNLS protein targeted to the outer surface of the ER; Fig. 4 *B* and *C*) (27).

As pharmacological treatments, we used α-amanitin, a highly specific and potent inhibitor of RNA polymerase II transcription, or a combination of pifithrin α, which selectively blocks p53-mediated transcription, and ADRIA to activate the remaining p53 pathways (28). As expected, we observed increased mitochondrial Ca^{2+} responses under both conditions (Fig. 4*A*), reflecting increased ER Ca^{2+} release and indicating a nontranscriptional role for p53 in Ca^{2+} modulation.

Moreover, the expression of p53-ΔNLS or ER-p53 chimeras in $p53^{-/-}$ MEF (Fig. 4*D*), HeLa (Fig. S5*A*), and H1299 (Fig. S5*B*) cells enhanced mitochondrial Ca^{2+} signaling, similar to the effect of p53 induction by ADRIA (Fig. 3*C*). This effect was further associated with a reestablished sensitivity to apoptosis induced by ER stress (Fig. 4*E*), as determined by cell count analysis (Fig. 4*F*) and PARP and caspase 3 cleavage (Fig. 4*G*).

In contrast, MDA-MB 468 cells, harboring the p53 273H mutant, were not sensitive to p53-ADRIA induction (Fig. 5*A*).

Accordingly, naturally occurring p53 mutants expressed in HCT-116 $p53^{-/-}$ cells (or in HeLa and H1299 cells; Fig. S5 *A* and *B*) lost their ability to increase the Ca^{2+} response (Fig. 5*B*).

Moreover, those mutants were unable to modulate Ca^{2+} homeostasis also failed to rescue the sensitivity to apoptosis after oxidative stress treatment (Fig. 5 *C*–*E*), although the apoptotic genes were expressed equally in cells expressing mutant p53 (Fig. S5*C*). A similar effect was observed when these mutations were introduced into p53-ΔNLS or ER-p53 chimeras (Fig. S6).

These data show that Ca^{2+}-mediated apoptosis is a transcription-independent pathway regulated by p53 at ER/MAMs.

p53 Modulates Ca^{2+} Homeostasis and Apoptosis by Interacting with the Sarco/ER Ca^{2+}-ATPase Pump at the ER, Changing Its Redox State. To dissect the mechanism by which WT p53 exerts its impact on Ca^{2+} homeostasis upon activation and accumulation at ER/MAM compartments, we examined whether p53 modulates the activity of sarco/ER Ca^{2+}-ATPase (SERCA) pumps, which mediate ER Ca^{2+} reaccumulation. Thus, we tested whether p53 functionally and physically interacts with SERCA. The in vitro interaction between p53 and endogenous SERCA was first detected using an MBP pull-down assay (Fig. 6*A* and Fig. S7*A*) in H1299 cells lacking p53, and the interaction was confirmed by the endogenous coprecipitation of the two proteins in WT MEFs (Fig. S7*B*). Next, we mapped the region of p53 involved in the interaction with SERCA. To this end, we used HA-tagged p53 deletion constructs: HAp53 1–175, HAp53 175–393, HAp53 294–393, and the full-length HA-p53. In coimmunoprecipitation experiments performed in H1299 cells transfected with the HA-p53 constructs, SERCA selectively bound to the C-terminal regulatory domain of p53, a region where posttranslational modifications can modify the interaction of p53 with partner proteins

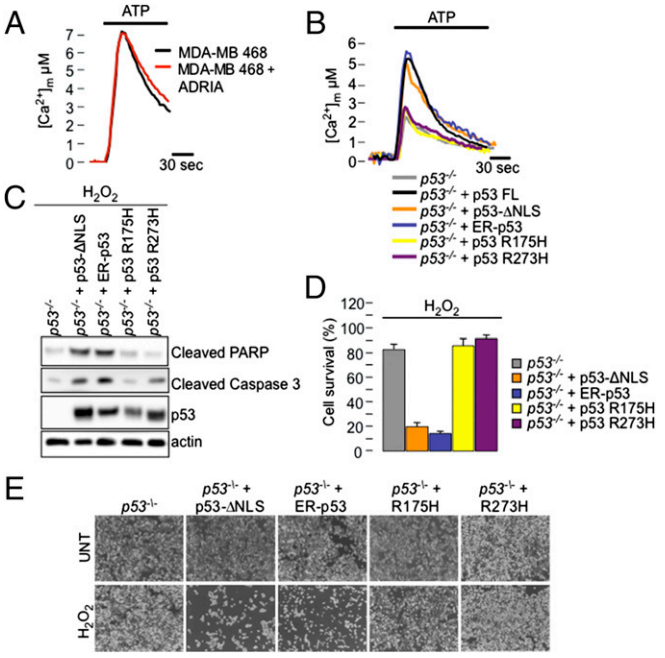

Fig. 5. p53 mutants cannot modulate the mitochondrial Ca^{2+} response and thus apoptosis. (*A*) Mitochondrial Ca^{2+} response after agonist stimulation in HCT-116 $p53^{-/-}$ cells and HCT-116 $p53^{-/-}$ cells after reintroduction of the p53-ΔNLS and ER-p53 chimeras or naturally occurring p53 mutants R175H and R273H. (*B*) Mitochondrial $[Ca^{2+}]$ after ATP stimulation measured in MDA-MB 468 cells, harboring p53 273H mutation, under control conditions and after adriamycin treatment (1 μM, 6 h). (*C* and *D*) Evaluation of apoptosis induction in HCT-116 $p53^{-/-}$ cells expressing p53-ΔNLS and ER-p53 chimeras or naturally occurring p53 mutants R175H and R273H after treatment with H_2O_2 using (*C*) immunoblot detection of cleaved PARP and cleaved caspase 3 (500 μM, 6 h) and (*D*) automated cell count analysis (500 μM, 12 h). Bars, SEM. (*E*) Representative images of HCT-116 $p53^{-/-}$ cells expressing different p53 constructs under untreated conditions and after H_2O_2 treatment (1 mM, 12 h).

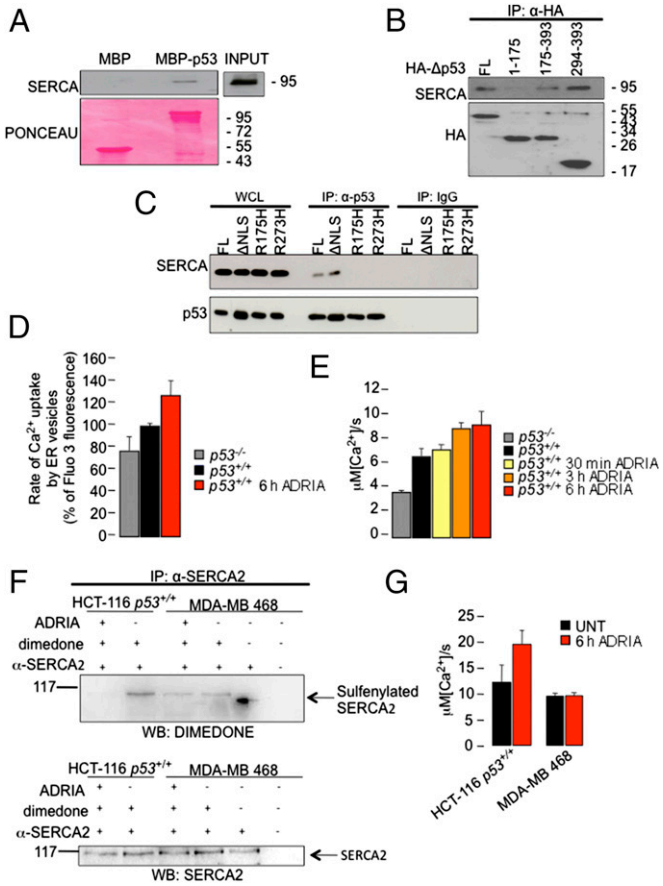

Fig. 6. p53 interacts with SERCA and stimulates Ca^{2+} accumulation in the ER, changing the SERCA oxidative state. (*A*) In vitro binding of endogenous SERCA to MBP-p53. H1299 cell lysates were incubated with bacterially expressed MBP-p53 protein or MBP as a control. Ponceau staining shows the amount of MBP proteins used in the experiments. (*B*) Full-length (FL) and HA-tagged p53 deletion mutants transiently expressed in H1299 cells were immunoprecipitated by anti-HA antibody and analyzed by Western blot (WB). IP, immunoprecipitation. (*C*) H1299 cells were transiently transfected with different p53 constructs (FL, full-length p53 WT; ΔNLS, p53-ΔNLS; R175H, p53 R175H; R273H, p53 R273H) and then harvested for immunoprecipitation and immunoblotting as indicated. WCL, whole cell lysate. (*D* and *E*) Rate analysis of Ca^{2+} uptake measured in the ER vesicles isolated from the (*D*) liver of $p53^{-/-}$ and $p53^{+/+}$ mice and $p53^{+/+}$ mice treated with adriamycin (1 μM, 6 h) or (*E*) ER compartments of $p53^{-/-}$ and $p53^{+/+}$ MEFs at different times after ADRIA (1 μM, 30 min, 3 h, 6 h) treatments. (*F*) Immunoblot with an antibody reactive to dimedone-conjugated cysteine residues of the protein sample extracts from HCT-116 $p53^{+/+}$ and MDA-MB 468 cells after ADRIA induction that were immunopurified using a monoclonal SERCA2 antibody. Cells with an active p53 reveal lower cysteinyl sulfenic acid-modified SERCA. (*G*) Analysis of ER Ca^{2+} uptake in HCT-116 $p53^{+/+}$ and MDA-MB 468 cells after ADRIA induction. Bars, SEM.

(Fig. 6*B* and Fig. S7*C*). However, the interacting fragment alone was not sufficient to modulate Ca^{2+} homeostasis and apoptosis (Fig. S7 *D* and *E*), suggesting that the entire p53 protein (or the majority of it) is required for its biological activity.

Interestingly, the naturally occurring p53 mutants R175H and R273H were unable to be coimmunoprecipitated with the SERCA protein. In contrast, the p53-ΔNLS protein retained this ability (Fig. 6*C*).

Finally, to establish whether p53 has a direct effect on SERCA activity, we analyzed the kinetics of ER Ca^{2+} accumulation both in vivo and in vitro. The Ca^{2+} accumulation rate was higher in the ER vesicles isolated from the liver of $p53^{+/+}$ mice treated intraperitoneally with ADRIA compared with those obtained from $p53^{+/+}$ and $p53^{-/-}$ mice (Fig. 6*D*). Similarly, the rate of ER Ca^{2+} accumulation, measured in MEFs, increased proportionally in a time-dependent manner with the induction of p53 by ADRIA, indicating a stimulatory role of p53 in SERCA activity (Fig. 6*E*), without affecting SERCA expression levels (Fig. S8*A*). These data were confirmed in HeLa cells overexpressing WT p53 and p53-NLS chimera (Fig. S8 *B* and *C*). To confirm the importance of SERCA activity in the Ca^{2+}-dependent apoptotic pathway, we evaluated the effect of SERCA overexpression on the Ca^{2+} response and cell death in $p53^{-/-}$ MEFs. We observed an increased mitochondrial Ca^{2+} uptake (Fig. S8*D*) that correlated with increased levels of cleaved caspase 3 upon H_2O_2 treatment (Fig. S8*E*), indicating that the activation of SERCA is sufficient to rescue the sensitivity to apoptosis in p53-deficient cells.

Next, we investigated the possible mechanism by which p53 stimulates SERCA activity upon binding. To this end, we analyzed whether p53 activation affects the oxidative state of the SERCA protein, which is known to modulate its activity (29). We thus compared the level of hyperoxidized sulfenylated proteins in HCT-116 $p53^{+/+}$ and MDA-MB 468 cells after the induction of WT p53 and mutant p53, respectively. Cells and lysates were exposed to dimedone, a chemical that selectively modifies sulfenylated cysteines, and the dimedone-modified proteins were detected by immunoblotting with an antibody to dimedone (30). In the absence of dimedone, the antibody gave a weak background signal (Fig. S9).

To understand whether the levels of sulfenylated SERCA were different in HCT-116 $p53^{+/+}$ and MDA-MB 468 cells, both cell types were exposed to dimedone to quench the sulfenylated cysteines, and the proteins were immunopurified using a monoclonal SERCA antibody. Immunoblotting of the SERCA immunocomplex with an antibody to dimedone revealed the presence of sulfenylated SERCA, which was lower in HCT-116 $p53^{+/+}$ cells treated with doxorubicin (Fig. 6*F*). In contrast, in MDA-MB 468 cells, SERCA oxidation was unchanged after ADRIA treatment. These results were then confirmed by measuring SERCA activity. Fig. 6*G* shows that ADRIA required WT p53 to be effective. Indeed, in MDA-MB 468 cells, SERCA activity was not sensitive to ADRIA induction of p53.

Discussion

In recent years, it has become evident that the ER, mitochondria, and region of close contact between these two organelles (MAMs) play a central role in different human diseases, including cancer (15, 31). One important process occurring in these intracellular domains is apoptosis.

A key signal transduction pathway connecting apoptosis to ER–mitochondrial interactions is an alteration in Ca^{2+} homeostatic mechanisms (32). The switch from a life to a death signal has been argued to occur when Ca^{2+} signaling between the ER and mitochondria is distorted, leading to a breakdown of mitochondrial function (9).

Interestingly, in recent years, many tumor suppressor proteins, such as PML (8), PTEN (33), Bax and Bak (34), BOK (35), PERK (36), ERO1α (37), and Bap31 and Fis1 (38), have been demonstrated to be localized to the ER and at MAMs, where they modulate cell death.

In the present study, we investigated whether p53 also shares this intracellular localization and whether, as for PML, PTEN, Bax, and Bak, p53 regulates apoptosis in a Ca^{2+}-dependent manner. p53 is a well-known tumor suppressor that coordinates different cell-death programs, mainly associated with its function as a transcription factor. Several studies have, however, described a transcription-independent function for p53, although the importance of the cytoplasmic pool of p53 for p53-mediated apoptotic cell death remains highly controversial.

We showed that a fraction of p53 is associated with the ER and MAMs. We demonstrated that this nonnuclear fraction of p53 is able to modulate Ca^{2+} homeostasis in response to both physiological and pathological stimulation. The activation and accumulation of p53 at ER/MAM compartments induced by anticancer drugs or stress allow apoptotic stimuli to rapidly and efficiently overload mitochondria with Ca^{2+}, a priming step for

the release of caspase cofactors and induction of apoptosis via the intrinsic pathway. As a consequence, cells are more prone to die through mitochondrial permeability transition pore opening (39), mitochondrial fragmentation, and cytochrome *c* release.

p53 present in the ER/MAM fraction physically interacts with SERCA, thus potentiating in vitro and in vivo Ca^{2+} accumulation in the ER lumen under stress conditions. In cancer cells, this proapoptotic mechanism is impaired due to the functional inactivation of p53, contributing to disease progression. In agreement with these results, SERCA overexpression, and thus its increased activity, and the subsequent ER Ca^{2+} overload have been previously demonstrated to increase spontaneous apoptosis (40). Our data suggest that the activation of WT p53 reduces the oxidation of SERCA (Fig. 6), thus modulating SERCA activity. Indeed, prooxidative modification of SERCA decreased its activity (29), and a critical cysteine in the SERCA sequence (41) that regulates this posttranslational modification is accessible from the cytosolic compartment (42), where p53 is localized.

Altogether, these results reveal a previously unidentified Ca^{2+}-dependent mechanism through which p53 exerts its potent proapoptotic role in response to anticancer treatments.

Materials and Methods

Reagents, solutions, cell culture, and transfection are described in *SI Materials and Methods*.

Detection of Cell Death. For cell-death induction, the cells were treated in complete medium as indicated in the text. Apoptosis was determined by different methods, as indicated in the text. Details are reported in *SI Materials and Methods*.

Calcium Measurements. Calcium analyses were performed by aequorin- (26), Fura-2–, and FRET-based measurements as specified in *SI Materials and Methods*.

Subcellular Fractionation. Fractionations were performed as described (19). IP3R, laminin, tubulin, and VDAC were used as markers.

SERCA Activity. The analysis of SERCA activity in vitro was obtained on traces performed with an aequorin targeted to the ER. The analysis of SERCA activity in vivo was obtained by the measurement of ER vesicle Ca^{2+} uptake in rectangular cuvettes using a spectrofluorimeter. Details are reported in *SI Materials and Methods*.

Detection of Sulfenylated SERCA2 in Cultured Cells. Proteins modified with sulfenic acid were detected following the procedure of Seo and Carroll (30).

Animals. Procedures involving animals and their care were in conformity with institutional guidelines and all experimental protocols were approved by the Animal Ethics Committee of Ferrara and Warsaw institutions.

ACKNOWLEDGMENTS. This study was supported by the Italian Association for Cancer Research (C.G., G.D.S., and P.P.); the Italian Ministry of Education, University and Research (COFIN, FIRB, and Futuro in Ricerca; G.D.S. and P.P.); NCI grants (to P.P.P.); Polish National Science Centre (UMO-2011/01/M/NZ3/02128); Polish Ministry of Science and Higher Education Grant W100/HFSC/2011 and Grant HFSP RGP0027/2011 (to M.R.W.); and a Telethon Career Award (TDEZ00112T; to E.Z.).

1. Green DR, Kroemer G (2009) Cytoplasmic functions of the tumour suppressor p53. *Nature* 458(7242):1127–1130.
2. Vousden KH, Lane DP (2007) p53 in health and disease. *Nat Rev Mol Cell Biol* 8(4):275–283.
3. Vogelstein B, Lane D, Levine AJ (2000) Surfing the p53 network. *Nature* 408(6810):307–310.
4. Marchenko ND, Wolff S, Erster S, Becker K, Moll UM (2007) Monoubiquitylation promotes mitochondrial p53 translocation. *EMBO J* 26(4):923–934.
5. Haupt S, Berger M, Goldberg Z, Haupt Y (2003) Apoptosis—The p53 network. *J Cell Sci* 116(Pt 20):4077–4085.
6. Moll UM, Wolff S, Speidel D, Deppert W (2005) Transcription-independent pro-apoptotic functions of p53. *Curr Opin Cell Biol* 17(6):631–636.
7. Sorrentino G, et al. (2013) The prolyl-isomerase Pin1 activates the mitochondrial death program of p53. *Cell Death Differ* 20(2):198–208.
8. Giorgi C, et al. (2010) PML regulates apoptosis at endoplasmic reticulum by modulating calcium release. *Science* 330(6008):1247–1251.
9. Giorgi C, De Stefani D, Bononi A, Rizzuto R, Pinton P (2009) Structural and functional link between the mitochondrial network and the endoplasmic reticulum. *Int J Biochem Cell Biol* 41(10):1817–1827.
10. Bernardi R, Papa A, Pandolfi PP (2008) Regulation of apoptosis by PML and the PML-NBs. *Oncogene* 27(48):6299–6312.
11. Rowland AA, Voeltz GK (2012) Endoplasmic reticulum-mitochondria contacts: Function of the junction. *Nat Rev Mol Cell Biol* 13(10):607–625.
12. Csordás G, et al. (2006) Structural and functional features and significance of the physical linkage between ER and mitochondria. *J Cell Biol* 174(7):915–921.
13. Giorgi C, et al. (2012) Mitochondrial Ca(2+) and apoptosis. *Cell Calcium* 52(1):36–43.
14. Hayashi T, Su TP (2007) Sigma-1 receptor chaperones at the ER-mitochondrion interface regulate Ca(2+) signaling and cell survival. *Cell* 131(3):596–610.
15. Pinton P, Giorgi C, Siviero R, Zecchini E, Rizzuto R (2008) Calcium and apoptosis: ER-mitochondria Ca^{2+} transfer in the control of apoptosis. *Oncogene* 27(50):6407–6418.
16. Sano R, et al. (2009) GM1-ganglioside accumulation at the mitochondria-associated ER membranes links ER stress to Ca(2+)-dependent mitochondrial apoptosis. *Mol Cell* 36(3):500–511.
17. Pinton P, Giorgi C, Pandolfi PP (2011) The role of PML in the control of apoptotic cell fate: A new key player at ER-mitochondria sites. *Cell Death Differ* 18(9):1450–1456.
18. Haupt Y, Rowan S, Shaulian E, Vousden KH, Oren M (1995) Induction of apoptosis in HeLa cells by *trans*-activation-deficient p53. *Genes Dev* 9(17):2170–2183.
19. Wieckowski MR, Giorgi C, Lebiedzinska M, Duszynski J, Pinton P (2009) Isolation of mitochondria-associated membranes and mitochondria from animal tissues and cells. *Nat Protoc* 4(11):1582–1590.
20. Costes SV, et al. (2004) Automatic and quantitative measurement of protein-protein colocalization in live cells. *Biophys J* 86(6):3993–4003.
21. Li J, Lee B, Lee AS (2006) Endoplasmic reticulum stress-induced apoptosis: Multiple pathways and activation of p53-up-regulated modulator of apoptosis (PUMA) and NOXA by p53. *J Biol Chem* 281(11):7260–7270.
22. Orrenius S, Zhivotovsky B, Nicotera P (2003) Regulation of cell death: The calcium-apoptosis link. *Nat Rev Mol Cell Biol* 4(7):552–565.
23. Mattson MP, Chan SL (2003) Calcium orchestrates apoptosis. *Nat Cell Biol* 5(12):1041–1043.
24. Akl H, Bultynck G (2013) Altered Ca(2+) signaling in cancer cells: Proto-oncogenes and tumor suppressors targeting IP3 receptors. *Biochim Biophys Acta* 1835(2):180–193.
25. Clapham DE (2007) Calcium signaling. *Cell* 131(6):1047–1058.
26. Bonora M, et al. (2013) Subcellular calcium measurements in mammalian cells using jellyfish photoprotein aequorin-based probes. *Nat Protoc* 8(11):2105–2118.
27. Yang M, Ellenberg J, Bonifacino JS, Weissman AM (1997) The transmembrane domain of a carboxyl-terminal anchored protein determines localization to the endoplasmic reticulum. *J Biol Chem* 272(3):1970–1975.
28. Vaseva AV, Moll UM (2009) The mitochondrial p53 pathway. *Biochim Biophys Acta* 1787(5):414–420.
29. Knyushko TV, Sharov VS, Williams TD, Schöneich C, Bigelow DJ (2005) 3-Nitrotyrosine modification of SERCA2a in the aging heart: A distinct signature of the cellular redox environment. *Biochemistry* 44(39):13071–13081.
30. Seo YH, Carroll KS (2009) Profiling protein thiol oxidation in tumor cells using sulfenic acid-specific antibodies. *Proc Natl Acad Sci USA* 106(38):16163–16168.
31. Raturi A, Simmen T (2013) Where the endoplasmic reticulum and the mitochondrion tie the knot: The mitochondria-associated membrane (MAM). *Biochim Biophys Acta* 1833(1):213–224.
32. Patergnani S, et al. (2011) Calcium signaling around mitochondria associated membranes (MAMs). *Cell Commun Signal* 9:19.
33. Bononi A, et al. (2013) Identification of PTEN at the ER and MAMs and its regulation of Ca(2+) signaling and apoptosis in a protein phosphatase-dependent manner. *Cell Death Differ* 20(12):1631–1643.
34. Scorrano L, et al. (2003) BAX and BAK regulation of endoplasmic reticulum Ca^{2+}: A control point for apoptosis. *Science* 300(5616):135–139.
35. Echeverry N, et al. (2013) Intracellular localization of the BCL-2 family member BOK and functional implications. *Cell Death Differ* 20(6):785–799.
36. Verfaillie T, et al. (2012) PERK is required at the ER-mitochondrial contact sites to convey apoptosis after ROS-based ER stress. *Cell Death Differ* 19(11):1880–1891.
37. Seervi M, Sobhan PK, Joseph J, Mathew KA, Santhoshkumar TR (2013) ERO1α-dependent endoplasmic reticulum-mitochondrial calcium flux contributes to ER stress and mitochondrial permeabilization by procaspase-activating compound-1 (PAC-1). *Cell Death Dis* 4:e968.
38. Iwasawa R, Mahul-Mellier AL, Datler C, Pazarentzos E, Grimm S (2011) Fis1 and Bap31 bridge the mitochondria-ER interface to establish a platform for apoptosis induction. *EMBO J* 30(3):556–568.
39. Bonora M, et al. (2013) Role of the c subunit of the FO ATP synthase in mitochondrial permeability transition. *Cell Cycle* 12(4):674–683.
40. Brini M, Bano D, Manni S, Rizzuto R, Carafoli E (2000) Effects of PMCA and SERCA pump overexpression on the kinetics of cell Ca(2+) signalling. *EMBO J* 19(18):4926–4935.
41. Qin F, et al. (2013) Hydrogen peroxide-mediated SERCA cysteine 674 oxidation contributes to impaired cardiac myocyte relaxation in senescent mouse heart. *J Am Heart Assoc* 2(4):e000184.
42. Bishop JE, Squier TC, Bigelow DJ, Inesi G (1988) (Iodoacetamido)fluorescein labels a pair of proximal cysteines on the Ca^{2+}-ATPase of sarcoplasmic reticulum. *Biochemistry* 27(14):5233–5240.